Iran J Sci Technol Trans Sci (2019) 43:1957–1965
https://doi.org/10.1007/s40995-018-0643-4

RESEARCH PAPER

Deposition of Ti6Al4V Thin Films by DC Magnetron Sputtering: Effect of the Current on Structural, Corrosion and Mechanical Properties

B. Abdallah[1] · M. Kakhia[1] · W. Alssadat[1] · M. S. Rihawy[1]

Received: 20 December 2017 / Accepted: 3 October 2018 / Published online: 17 October 2018

Abstract
Ti6Al4V films have been prepared by DC magnetron sputtering technique at different currents (600, 700, 800 and 900 mA); target–substrate distance has been 3 cm. The depositions were carried out from Ti6Al4V alloy target. The deposition rate increases with increasing the current. The current effect on the crystalline quality and texture has been investigated by means of X-ray diffraction. β-Phase has been identified, and the grain size has been found to increase with increasing the current. The composition of the films has been determined by proton-induced X-ray emission and Rutherford backscattering technique. The Ti ratio was found to increase with current. The results obtained indicate that the TiAlV films by DC magnetron sputtering can inhibit the aggressive action of corrosion media. With increasing the current to improve film quality (bigger grain size), film Ti6Al4V/SS304 improved corrosion resistance for 304 substrate; microhardness was measured using Vickers method by applying 10 g load. Ti6Al4V film improves corrosion resistance and microhardness.

Keywords Ti6Al4V film · DC magnetron sputtering · PIXE · XRD · Corrosion

1 Introduction

Titanium alloys are widely utilized for a variety of applications and have been comprehensively investigated (Yamada 1996; Gorynin 1999; Gurrappa 2003; Faria et al. 2011), owing to their well-known interesting chemical and mechanical properties (Metikoš-Hukovic et al. 2003) compared with pure titanium. The titanium element is a monophase metal, physiologically inert, and non-toxic.

Most applications of titanium involve mixing it with small amounts of aluminum and vanadium, typically 6% and 4%, respectively, by weight, to form a metallic alloy, which is normally indicated as Ti6Al4V. This ternary titanium alloy exhibits α and β phases structure, with enhanced mechanical properties, high resistance to corrosion and wear and good hardness and tenacity (Aragon and Hulbert 1972; Khan et al. 1996; Akahori and Niinomi 1998; Long and Rack 1998; Torres et al. 2001). These features enable effective utilization of such alloy in many applications, especially those associated with biological systems. It is widely used in the fabrication of medical implants due to its excellent biocompatibility (Roessler et al. 2002; Dimcic et al. 2004; Faria et al. 2011). Zhang et al. (2015) have investigated microstructure, microhardness and corrosion performance of Ti6Al4V alloy. Also, these alloys are widely applied for dental and orthopedic implants due to their biocompatibility (Krischok et al. 2007; Variola et al. 2008; Yildiz et al. 2009). They provide higher biomechanical properties and chemical stability in biological systems than other materials such as stainless steel and cobalt–chromium alloys (Chang-bin et al. 2011).

The use of material as medical implant includes study of corrosion resistance in physiological solution, like 0.9% NaCl solution, which simulates the environment of the blood plasma (Barril et al. 2005). Surface treatment is widely used to enhance abrasion, corrosion resistance and surface hardness (Wang et al. 2010). Nitriding is often used to harden the titanium alloy surface (Budzynski et al. 2006). Good biocompatibility of titanium nitride is shown in the blood and bone tissue (Subramanian et al. 2011). In addition, the titanium nitride is characterized by good

✉ B. Abdallah
pscientific27@aec.org.sy

[1] Department of Physics, Atomic Energy Commission, P. O. Box 6091, Damascus, Syria

mechanical, tribological and anticorrosion properties; that is why, the titanium nitride is the most suitable to protect the surface of medical implants.

Surface-modified Ti6Al4V alloy is generally used as a suitable substrate. A nanostructured surface layer of Ti6Al4V alloy was obtained by ultrasonic shot peening (USSP) (Zhang et al. 2015). Subsequently, the corrosion performance was investigated using potentiodynamic polarization and electrochemical impedance spectroscopy (EIS). A few studies have applied this alloy as thin film; for instance, in previous work, we have demonstrated a successful preparation of TiAlV films by vacuum arc discharge technique starting from Ti, Al and V elemental targets (Abdallah et al. 2013a). The effect of temperature on the composition and crystalline quality has been investigated. The films composition is found to be similar to the standard Ti6Al4V alloy. Increasing the temperature has caused an increase in the Ti ratio and enhancement in the texture of the films.

Other preparation techniques have also been used to deposit thin films of Ti6Al4V, for example chemical vapor deposition (CVD) or physical vapor deposition (PVD), such as reactive magnetron sputtering (Luo 2011), RF sputtering (Alfonso et al. 2006) and DC magnetron sputtering (Li et al. 2013). There are a few studies that utilize the DC magnetron sputtering using Ti6Al4V target.

In this work, TiAlV films have been deposited on Si and stainless steel (SS304) substrates by DC magnetron sputtering method using different current values. The crystallographic properties of the films were studied by XRD technique. The microhardness was investigated using Vickers method. In addition, the elemental composition of the films was obtained by PIXE, EDX and RBS techniques. The corrosion performance was investigated using potentiodynamic polarization.

2 Experimental Details

The films were prepared by a DC magnetron sputtering system starting from highly pure (99.99%) Ti6Al4V target (Al 6 wt%, V 4 wt% and balance Ti) of 50 mm diameter. A cylindrical high-vacuum chamber (Fig. 1), made of stainless steel 316, 363 mm diameter and 492 mm height, was fabricated locally. A turbo-molecular pump was installed. The films were deposited on Si (100), SS304 and carbon substrates within an argon discharge for 10 min. The distance between the target and the substrate was 3 cm. The residual pressure was lower than 2×10^{-6} Torr, and the working pressure was about 2.2 mTorr with argon flux 17 sccm. The substrate was rotated continuously around the vertical central axis 20 rpm. During deposition,

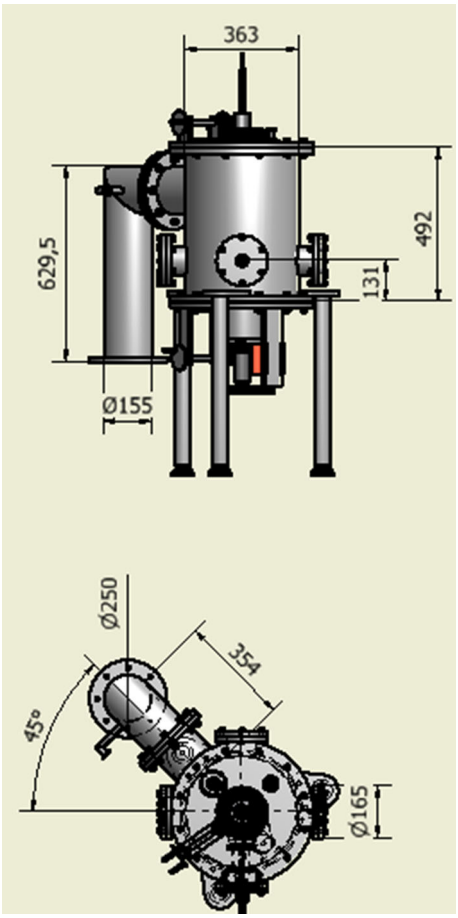

Fig. 1 Diagram of DC magnetron sputtering system

the plasma current was varied 600, 700, 800 and 900 mA (from 230 W to 350 W power) at room temperatures.

The crystallographic properties of the prepared films were studied by X-ray diffraction (Stoe StadiP transmission X-ray diffractometer). Films thickness was obtained with a Tescan Vega II XMU scanning electron microscope (SEM) equipped with energy-depressive X-ray spectroscopy (EDX), which has been used for determination of the elemental composition of the prepared samples.

The elemental composition of the films on carbon substrate was measured using the PIXE technique. The measurements were taken using 2 MeV proton beam produced from the 3MV HVEE^{TM} tandem accelerator at the Atomic Energy Commission of Syria (AECS). Ti6Al4V target (99.99%) reference target has been used to validate and calibrate the PIXE measurements. A detailed characterization of the PIXE system is previously reported in (Rihawy et al. 2016). The RBS analysis was performed using alpha beam of energy of 2.0 MeV that hits the samples normally with a total dose of approximately 5 μC. Backscattered particles were detected at 170° using

passivated ion-implanted detector (PIPS) with resolution of 12 keV.

Microhardness measurements were taken using a HX-1000 microhardness tester with Vickers indenter at loading force of 10 g force (gF) with the time of indentation kept constant at 15 s.

2.1 Corrosion Test (Electrochemical Test)

The electrochemical corrosion test was carried out using conventional three-electrode cell of 300 ml capacity by using Voltalab PGZ 301 (France) and Tafel extrapolation method. The cell was fitted with working electrode, saturated calomel electrode (SCE) as the reference electrode and the platinum as a counter electrode. The studies were carried out in normal saline (0.9% NaCl) solution at 37 ± 1 °C with scan rate 0.166 mV/s, and electrode potential was raised from − 800 to 1000 mV. The critical parameters like E_{corr}, I_{corr} and corrosion rate in mm/year were evaluated from the Tafel plots.

3 Results and Discussion

3.1 Deposition Rate and RBS Analysis

Figure 2a shows increase in the deposition rate with the increase of the current. The deposition current was the main factor influencing the deposition rate as demonstrated by Farooq and Lee (2002), because of the increase in the ionic bombardment. It is worth mentioning that other factors affect the deposition rate, like the increase in the oxygen or nitrogen ratios (Rizzo et al. 2007; Abdallah et al. 2013b, 2017; Naddaf et al. 2016) that decrease the deposition rate. The RBS measurements (Fig. 2b) confirm the behavior shown by deposition rate measurements, where the thickness of the films increases with the current, as peak width is associated with the film thickness (Ismail et al. 2012).

Figure 2c shows SEM cross section for film/Si deposited at 900 mA, where the thickness of the film is 850 nm and the deposition rate is 85 nm/min.

3.2 Structural Characterization (XRD)

Figure 3a shows the XRD patterns of the Ti6Al4V films. The highest intensity peak is symmetric and can be assigned to β-phase of Ti(110) at about 38.48°, where β-phase in PDF number: 44-1288 **a =** 3.3065 Å, similar to the results of the TiAlV films deposited by RF sputtering (Garzón et al. 2014). As shown in Fig. 3a, peak position has been varied from 37.69° to 38.24° when current increased from 600 to 900 mA. This shift indicates decrease in residual stress with current because the peak position for our massif target (zero stress) was 38.53° at (110) orientation. The α-phase of Ti(002) is not clearly shown in these films; however, we have observed both phases (α and β) in a previous work (Abdallah et al. 2013a), where vacuum arc deposition technique was applied.

The grain size was then calculated using Scherrer's formula (Scherrer 1918) for the films and is presented in Fig. 3b, where the average grain size is increased with current. The intensities of these peaks become higher and sharper with increasing the current (Fig. 3a). This suggests that the crystallinity of the resulting films is improved and the crystallite sizes become larger as justified by calculated values, possibly as a result of increase in the deposition rate with current. Li et al. (2013) demonstrated change in orientation direction form (102) to (002) at room temperature and at 300 °C, respectively. They have noticed that smaller grain size is obtained at higher temperature.

It has been reported that the grain size plays crucial role in corrosion behavior and wear resistance and mechanical properties (hardness and elastic modulus) (Wang et al. 2006a; Mao et al. 2011; Unal et al. 2014).

3.3 Composition Analysis (PIXE + EDX)

The elemental composition of the films has been obtained by means of both EDX and PIXE techniques (Fig. 4a, b). X-ray peaks of Ti, Al and V are clearly shown on EDX spectra for the prepared film at 900 mA. Table 1 shows that the Ti percentage was about 85.31 wt%. This result justified that the film composition was close to Ti4Al6V standard. The percentage obtained of 79.59 at.% for Ti is nearly similar to that found by Alfonso et al. (2006) for films prepared by RF sputtering method starting from a Ti6Al4V target.

Patsalas et al. (2000) have demonstrated that under the used experimental conditions, the sputtering rates of Ti, Al and V were slightly different, which result in difference in stoichiometry between the prepared films and the target.

Figure 4b shows two overlaid PIXE spectra of TiAlV film (deposited on C substrate) prepared at 900 mA and Ti6Al4V target. Both spectra are almost identical, which demonstrates similar composition. Si and K traces are shown in the spectra due to sample handling and preparation. The peak shown at 2.76 keV is assigned to the escape peak of K_α X-rays of Ti.

The Ti percentage (wt%) evolution in the films was calculated using PIXE (Fig. 4c) technique, following comprehensive calibrations procedures (Rihawy et al. 2016). It is clear that the Ti percentage increased with the current. The stoichiometry of the films was influenced by the current value. It is worth mentioning that composition

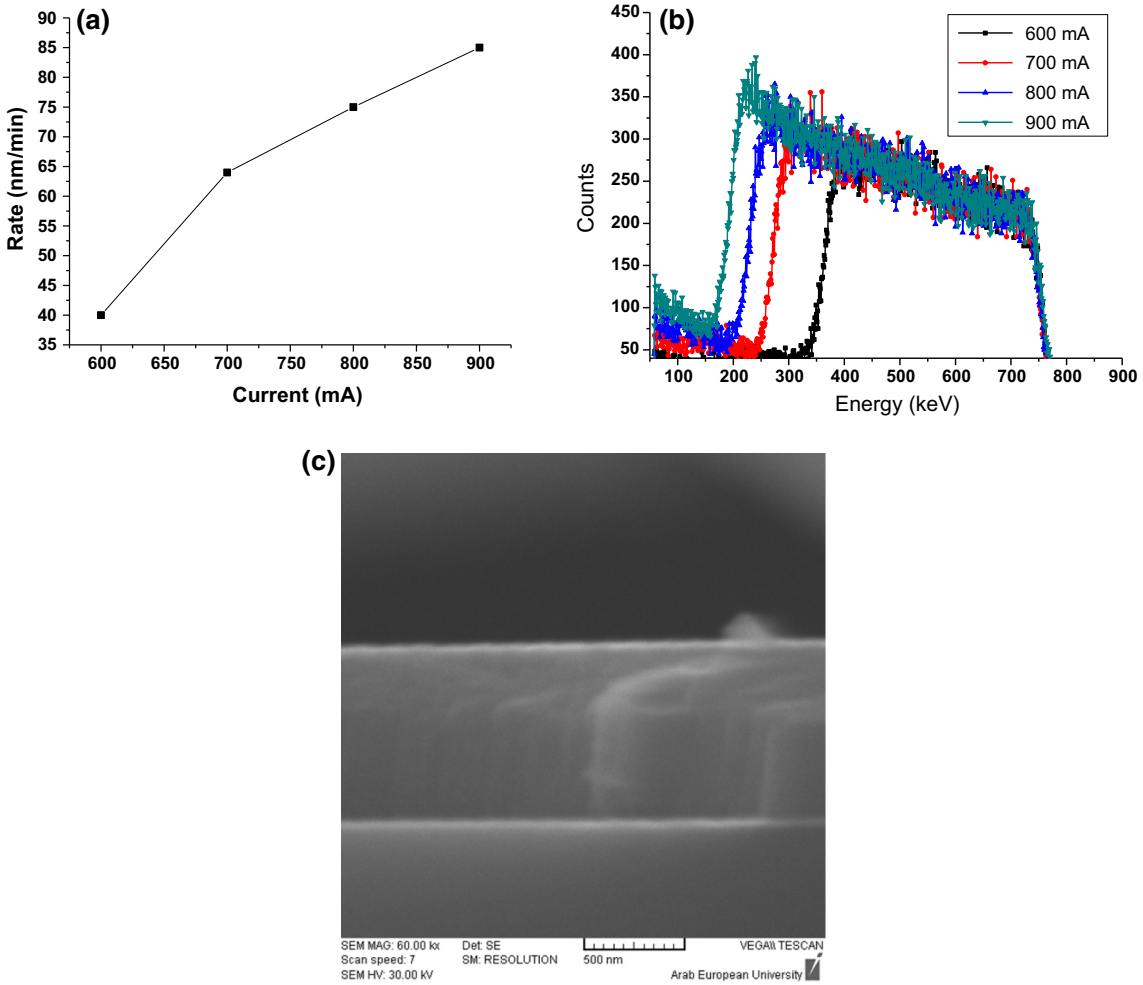

Fig. 2 **a** Deposition rate and **b** Rutherford backscattering spectra for TiAlV film as a function of the current and **c** SEM cross section for film deposited at 900 mA

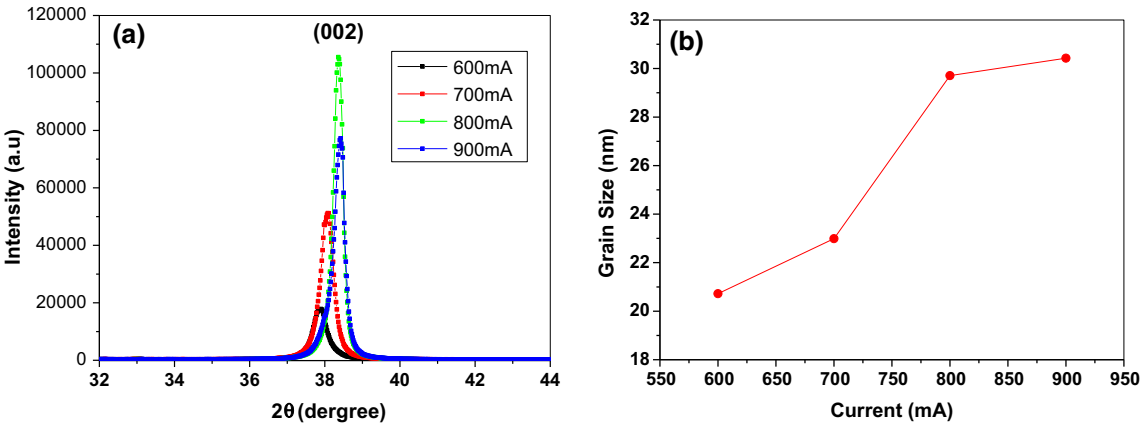

Fig. 3 **a** XRD pattern and **b** grain size for TiAlV/Si film as a function of the current

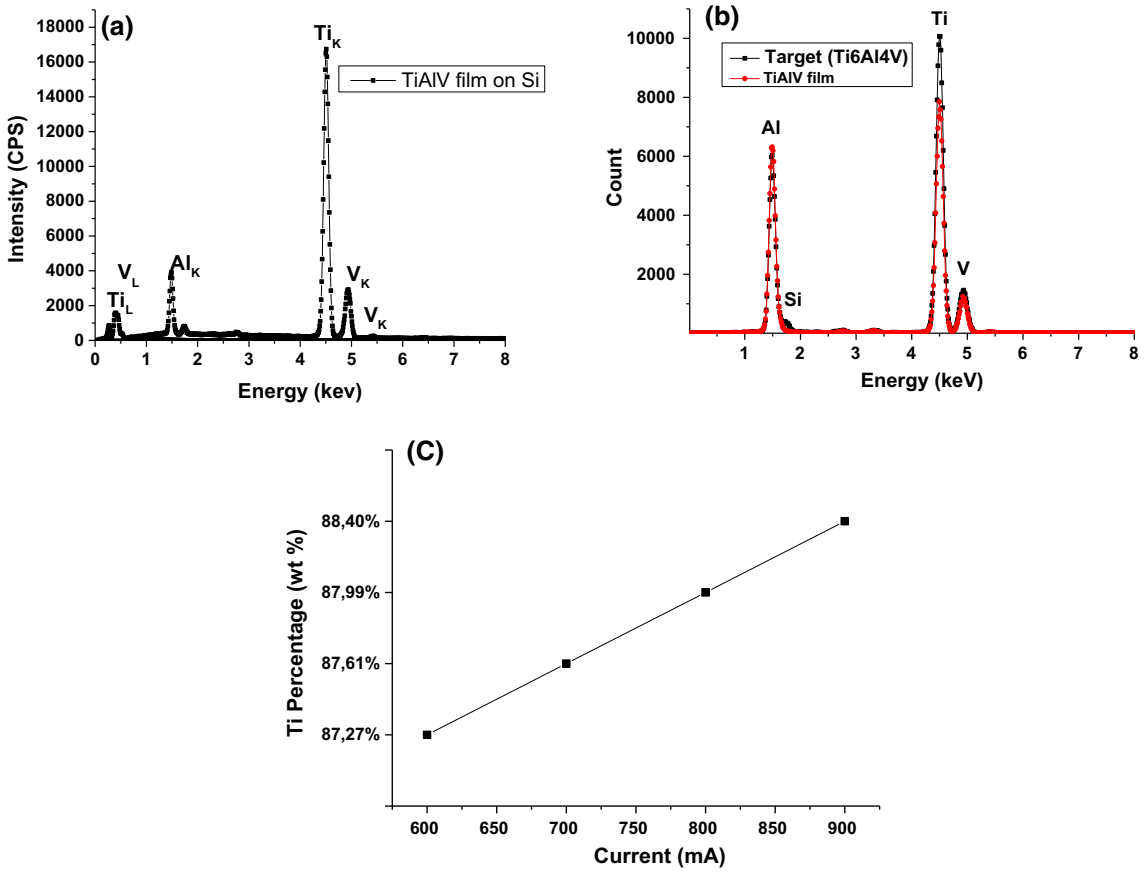

Fig. 4 **a** EDX spectrum for TiAlV film deposited at 900 mA and **b** two overlaid PIXE spectra for both target and TiAlV film deposited on carbon substrate at 900 mA and **c** the evaluation of Ti percentage obtained by PIXE as a function of the current

Table 1 EDX result (weight and atomic percentage) for TiAlV/Si film deposited at 900 mA

	wt%	at.%
Al_K	9.65	15.99
Ti_K	85.31	79.59
V_K	5.04	4.42

values obtained by EDX are in good agreement with PIXE ones.

3.4 Microhardness Measurements

The microhardness measurements were taken for the films/Si using a small loading force value (10 gF), because larger load values could be influenced by the substrate hardness, where the thickness of the films is less than 1 μm. The value of Vickers microhardness decreases from 6.2 to 4.2 GPa with increase of the current from 600 to 900 mA. It is noteworthy to mention that the larger value of the microhardness corresponds to the smaller grain size, where at low current value (600 mA) a small grain size was obtained ($\sim$ 21 nm) (see Fig. 3b). This behavior between the grain size and the microhardness was previously reported by (Huang et al. 2007; Abdallah et al. 2013a). The hardness of titanium alloy (bulk Ti6Al4V) is about 3.6 GPa (Ashby and Jones 1980), while Si substrate hardness is 9 GPa (Bhattacharya and Nix 1988).

The microhardness values of the TiAlV films found in the literature varied from 4 to 11 GPa (Leng et al. 2000; Clem et al. 2006; Pawlak and Wendler 2009; Costa et al. 2010). Our measurements presented in this work are smaller than those reported in the previous work of TiAlV films (Abdallah et al. 2013a), prepared by vacuum arc deposition, about few GPa. This arises due to the difference synthesis techniques, where the energy of ionic bombardment in vacuum arc is higher (< 150 eV) than the sputtering bombardment energy (< 50 eV), and/or due to the existence of two phases α/β in films prepared by vacuum arc technique while only a priori β-phase was found (BCC titanium phase) by sputtering technique (Fig. 5).

Garzón et al. (2014) obtained average nanohardness varied from 8.5 to 10 GPa for Ti6Al4V films prepared by RF magnetron sputtering. This difference could be due, as we believe, to the difference in synthesis technique between RF and DC sputtering, because the energy bombardment in DC was less than RF sputtering and/or their

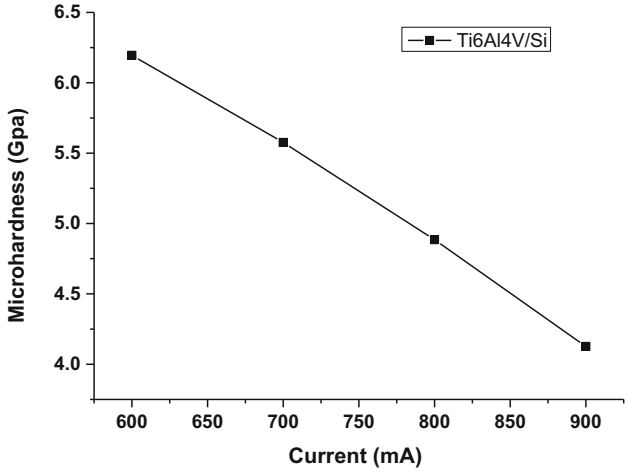

Fig. 5 Microhardness evaluation for films deposited on Si substrate as a function of the current

Table 2 Corrosion rate of Ti6Al4V film and SS304 by Tafel extrapolation method in 0.9% NaCl solution at 37 °C

	I_{corr} (μA/cm^2)	E_{corr} (mV)
SS304	84.25	− 454.3
900 mA	4.44	− 90.6
800 mA	3.72	− 190.6
700 mA	1.68	+ 66.3
600 mA	1.47	+ 178.7

film (Garzón et al. 2014) have small average grain size (11–16 nm).

3.5 Corrosion Measurements

The characteristic electrochemical parameters in Tafel method (Frankel 2016) include corrosion potential (E_{corr}) and corrosion current density (I_{corr}). The corrosion current density attained from the polarization curves is usually proportional to the corrosion rate (Wang et al. 2006b). The corrosion resistance of Ti6Al4V deposited on SS304 in normal saline solution was studied and compared with uncoated SS304 sample. The present study showed that Ti6Al4V/SS304 film had lower corrosion rate compared with 304 stainless steel in normal saline solution.

The corrosion resistance of the sample has been enhanced in comparison with the reference (SS304). All the coated samples showed higher corrosion potential E_{corr}, lower corrosion current density I_{corr} and lower corrosion rate than the uncoated samples.

Pohrelyuk et al. (2013) has demonstrated, for nitride Ti6Al4V alloys, that I_{corr} (μA/cm^2) of both thin and thick films is varied between 6 and 15, respectively, when 0.9% NaCl was used at 36 °C. Recent studies have shown that grain size is a critical factor in the corrosion resistance of metallic materials and mechanical properties (Wang et al. 2006a; Mao et al. 2011; Unal et al. 2014), where smaller grain size is associated with better corrosion resistance.

Table 2 shows I_{corr}, E_{corr} and corrosion rate for both SS304 and films. It is clear that I_{corr} values decrease from 84.25 μA/cm^2 for SS304 to 1.47 μA/cm^2 for film prepared at 600 mA.

All samples exhibit an anodic shift in E_{corr} and a significant decrease in I_{corr} as shown in Fig. 6a, corresponding to enhanced corrosion resistance. This behavior could be due to the decrease in the grain size values (Fig. 3b) where better corrosion resistance is obtained for the sample prepared at low current (600 mA).

Figure 6a shows potentiodynamic polarization curves of SS304 substrate and Ti6Al4V films deposited on SS304 in 0.9% NaCl at 37 °C. It can be seen that corrosion properties have been improved as mentioned above. The smallest corrosion current density corresponding to the best corrosion properties was obtained for the Ti6Al4V film prepared at

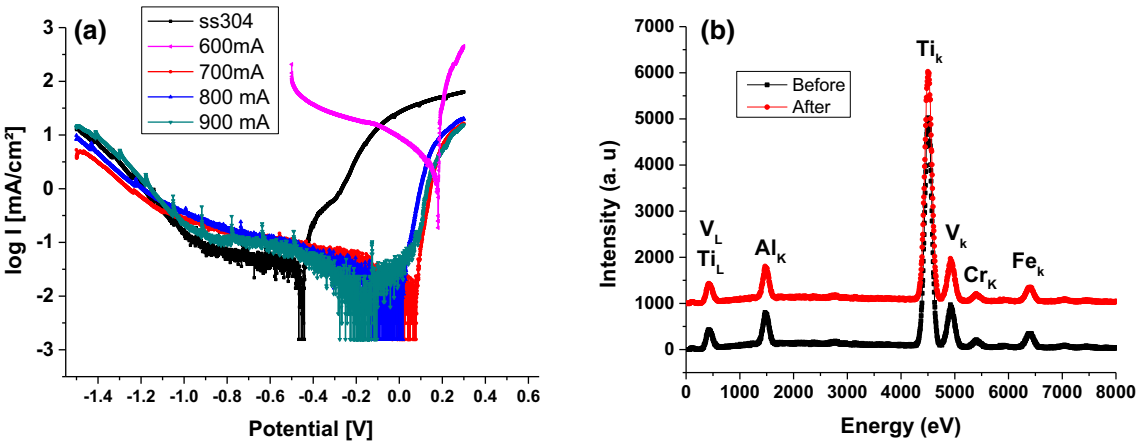

Fig. 6 **a** Potentiodynamic polarization curves of SS304 substrate and Ti6Al4V films deposited on SS304 in 0.9% NaCl at 37 °C and **b** EDX spectra of film on SS304 deposited at 600 mA before and after corrosion test

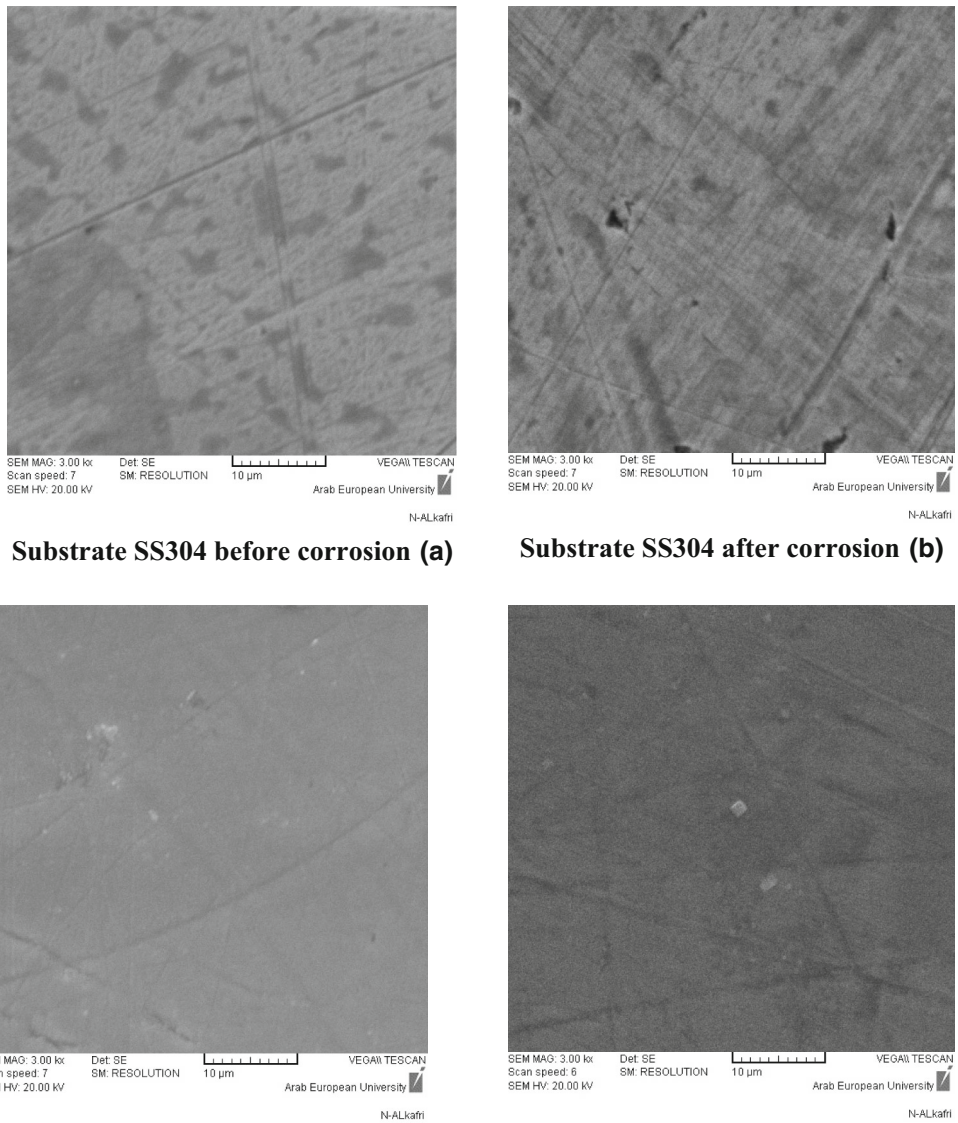

Fig. 7 SEM images of **a** and **b** substrate SS304 before and after corrosion, respectively, and **c** and **d** film deposited at 600 mA before and after corrosion, respectively

600 mA. A positive value of the corrosion potential is an indicator of low electrochemical activity that is associated with good corrosion resistance (Kalisz et al. 2016).

Figure 6b shows two EDX overlaid spectra of the film prepared at 600 mA, before and after corrosion test, have shown no considerable change for the corresponding (weight and atomic) percentage values for Ti, V and Al elements.

The composition of the passive film formed on the deposits is rather complex since it contains several forms of oxidized titanium and vanadium as well as Al_2O_3. We have found in a previous work, where X-ray photoelectron spectroscopy (XPS) was used to study the chemical composition of the passive layer formed on the films deposited by vacuum arc discharge method, that this layer was mainly composed of TiO_2 (Abdallah et al. 2013a). The formation of "protective" oxide TiO_2 layer on the surface of film results in excellent corrosion resistance in various test solutions and physiological media (Al-Mayouf et al. 2004; Goldberg and Gilbert 2004), giving that this oxide layer is considered as a barrier between the surrounding environment and the underlying metallic titanium. Many factors could influence corrosion behavior such as TiO_2 phase, defect density, stoichiometry, preferred orientation, α/β phases and grain size (Musil 2000).

It has been reported that refinement of grain size has remarkable enhancement in the corrosion resistance (op't Hoog et al. 2008; Aung and Zhou 2010). This agrees with our

results where the grain size decreases with the decrease in the current value (from 900 to 600 mA), as can be seen in Fig. 6a.

3.6 Surface Morphology

Figure 7 shows SEM surface morphology of substrate SS304 before (a) and after (b) corrosion, respectively. The lines, which appear as sharp edges, are resulting due to paper polishing of SS304 (a–b). Pitting corrosion as well as unsharp edges is clearly shown after corrosion test.

Figure 7c, d for film deposited at 600 mA before and after corrosion, respectively, shows less corrosion effect compared with uncoated substrate, which is consistent with the Tafel curve.

Our films have nanocrystalline size, which varies with the experimental parameters, which is associated with high-density grain boundaries of the nanocrystalline material, which make the impurity uniformly distributed and enhance the passive film formation. Balusamy et al. (2010) and Zhang et al. (2015) expressed a similar viewpoint. The corrosion–electrochemical behavior is normally associated with a change of the dominant processes of oxidation–reduction reaction by increasing the surface roughness (Pohrelyuk et al. 2013).

This study has shown that TiAlV film deposited on SS304, by DC magnetron sputtering, can potentially be applied as a successful biomaterial. Few studies have utilized these films by this technique in place of the conventional alloys. They exhibit accepted inhibition against the aggressive action of corrosion media. Additionally, the low-cost aspect can be efficiently considered.

4 Conclusion

Ti6Al4V films have been prepared by DC magnetron sputtering technique at different current values (power). The depositions were carried out from Ti6Al4V targets. The current effects on the crystalline quality and texture have been investigated by means of X-ray diffraction. β-phase has been identified, and the grain size has been found to increase with current. The composition of the films has been determined by proton-induced X-ray emission technique. The effect of current on the composition and crystalline quality has been investigated. The films composition is found to be getting to the standard Ti6Al4V alloy. Increasing the current permitted to increase the Ti ratio and to enhance the texture of the films. The microhardness of the films was found to decrease with the current and to be slightly larger than literatures values. The Ti ratio was found to increase with current. The microhardness measured by the Vickers indentation method was found to decrease with current. EDX and PIXE were used to study the chemical composition of the films. They indicate that prepared films prevent the aggressive action of corrosion media. Therefore, the Ti6Al4V film is an effective method to improve the corrosion resistance of SS304.

Acknowledgements The authors would like to thank Prof. Dr. I. Othman the Director General of the Atomic Energy Commission of Syria.

References

Abdallah B, Mrad O, Ismail IM (2013a) Characterization of TiAlV films prepared by vacuum arc deposition: effect of substrate temperature. Acta Phys Pol, A 123(1):76–79

Abdallah B, Naddaf M, A-Kharroub M (2013b) Structural, mechanical, electrical and wetting properties of ZrNx films deposited by Ar/N2 vacuum arc discharge: effect of nitrogen partial pressure. Nucl Instrum Methods Phys Res Sect B Beam Interact Mater Atoms 298:55–60

Abdallah B, Jazmatia AK, Refaaia R (2017) Oxygen effect on structural and optical properties of ZnO thin films deposited by RF magnetron sputtering. Mater Res 20:607–612

Akahori T, Niinomi M (1998) Fracture characteristics of fatigued Ti–6Al–4V ELI as an implant material. Mater Sci Eng, A 243(1–2):237–243

Alfonso JE, Torres J, Marco JF (2006) Influence of the substrate bias voltage on the crystallographic structure and surface composition of Ti6A14V thin films deposited by rf magnetron sputtering. Braz J Phys 36:994–996

Al-Mayouf A, Al-Swayih A, Al-Mobarak N (2004) Effect of potential on the corrosion behavior of a new titanium alloy for dental implant applications in fluoride media. Mater Corros 55(2):88–94

Aragon PJ, Hulbert SF (1972) Corrosion of Ti–6Al–4V in simulated body fluids and bovine plasma. J Biomed Mater Res 6(3):155–164

Ashby MF, Jones DRH (1980) Engineering materials. Pergamon, Oxford

Aung NN, Zhou W (2010) Effect of grain size and twins on corrosion behaviour of AZ31B magnesium alloy. Corros Sci 52(2):589–594

Balusamy T, Kumar S, Sankara Narayanan TSN (2010) Effect of surface nanocrystallization on the corrosion behaviour of AISI 409 stainless steel. Corros Sci 52(11):3826–3834

Barril S, Mischler S, Landolt D (2005) Electrochemical effects on the fretting corrosion behaviour of Ti6Al4V in 0.9% sodium chloride solution. Wear 259(1–6):282–291

Bhattacharya AK, Nix WD (1988) Finite element simulation of indentation experiments. Int J Solids Struct 24(9):881–891

Budzynski P, Youssef AA, Sielanko J (2006) Surface modification of Ti–6Al–4V alloy by nitrogen ion implantation. Wear 261(11–12):1271–1276

Chang-bin T, Dao-xin L, Zhan W, Yang G (2011) Electro-spark alloying using graphite electrode on titanium alloy surface for biomedical applications. Appl Surf Sci 257(15):6364–6371

Clem WC, Konovalov VV, Chowdhury S, Vohra YK, Catledge SA, Bellis SL (2006) Mesenchymal stem cell adhesion and spreading on microwave plasma-nitrided titanium alloy. J Biomed Mater Res, Part A 76(2):279–287

Costa MYP, Cioffi MOH, Voorwald HJC, Guimarães VA (2010) An investigation on sliding wear behavior of PVD coatings. Tribol Int 43(11):2196–2202

Dimčić B, Bobić I, Maksimović V, Mišković Z, Zec S (2004) C0068aracterization of a hard surface layer (» α case «) on Ti–6Al–4V surgical implants. Assoc Metall Eng Serbia Monten 10:255–260

Faria ACL, Rodrigues RCS, Claro APRA, de Mattos MGC, Ribeiro RF (2011) Wear resistance of experimental titanium alloys for dental applications. J Mech Behav Biomed Mater 4(8):1873–1879

Farooq M, Lee ZH (2002) Optimization of the sputtering process for depositing composite thin films. J Korean Phys Soc 40(3):511–515

Frankel GS (2016) Fundamentals of corrosion kinetics. In: Hughes AE, Mol JMC, Zheludkevich ML, Buchheit RG (eds) Active protective coatings: new-generation coatings for metals. Springer, Dordrecht, pp 17–32

Garzón CM, Alfonso JE, Corredor EC (2014) Characterization of adherence for Ti6Al4V films RF magnetron sputter grown on stainless steels. Dyna 81(185):7

Goldberg JR, Gilbert JL (2004) The electrochemical and mechanical behavior of passivated and TiN/AlN-coated CoCrMo and Ti6Al4V alloys. Biomaterials 25(5):851–864

Gorynin IV (1999) Titanium alloys for marine application. Mater Sci Eng, A 263(2):112–116

Gurrappa I (2003) Characterization of titanium alloy Ti–6Al–4V for chemical, marine and industrial applications. Mater Charact 51(2–3):131–139

Huang J-H, Ho C-H, Yu G-P (2007) Effect of nitrogen flow rate on the structure and mechanical properties of ZrN thin films on Si(1 0 0) and stainless steel substrates. Mater Chem Phys 102(1):31–38

Ismail IM, Abdallah B, Abou-Kharroub M, Mrad O (2012) XPS and RBS investigation of TiNxOy films prepared by vacuum arc discharge. Nucl Instrum Methods Phys Res, Sect B 271:102–106

Kalisz M, Grobelny M, Świniarski M, Mazur M, Wojcieszak D, Zdrojek M, Judek J, Domaradzki J, Kaczmarek D (2016) Comparison of structural, mechanical and corrosion properties of thin TiO_2/graphene hybrid systems formed on Ti–Al–V alloys in biomedical applications. Surf Coat Technol 290:124–134

Khan MA, Williams RL, Williams DF (1996) In-vitro corrosion and wear of titanium alloys in the biological environment. Biomaterials 17(22):2117–2126

Krischok S, Blank C, Engel M, Gutt R, Ecke G, Schawohl J, Spieß L, Schrempel F, Hildebrand G, Liefeith K (2007) Influence of ion implantation on titanium surfaces for medical applications. Surf Sci 601(18):3856–3860

Leng YX, Chen JY, Zeng ZM, Tian XB, Yang P, Huang N, Zhou ZR, Chu PK (2000) Properties of titanium oxide biomaterials synthesized by titanium plasma immersion ion implantation and reactive ion oxidation. Thin Solid Films 377–378:573–577

Li L, Li WX, Zeng LY, Yang Y, Hou ZM, Han D (2013) Effect of deposition temperature on the structure and mechanical properties of Ti–6Al–4V film. Mater Sci Forum 749:643–647

Long M, Rack HJ (1998) Titanium alloys in total joint replacement—a materials science perspective. Biomaterials 19(18):1621–1639

Luo Q (2011) Temperature dependent friction and wear of magnetron sputtered coating TiAlN/VN. Wear 271(9–10):2058–2066

Mao XY, Li DY, Fang F, Tan RS, Jiang JQ (2011) Application of a simple surface nanocrystallization process to a Cu–30Ni alloy for enhanced resistances to wear and corrosive wear. Wear 271(9–10):1224–1230

Metikoš-Huković M, Kwokal A, Piljac J (2003) The influence of niobium and vanadium on passivity of titanium-based implants in physiological solution. Biomaterials 24(21):3765–3775

Musil J (2000) Hard and superhard nanocomposite coatings. Surf Coat Technol 125(1–3):322–330

Naddaf M, Abdallah B, Ahmad M, A-Kharroub M (2016) Influence of N_2 partial pressure on structural and microhardness properties of TiN/ZrN multilayers deposited by Ar/N_2 vacuum arc discharge. Nucl Instrum Methods Phys Res, Sect B 381:90–95

Op't Hoog C, Birbilis N, Estrin Y (2008) Corrosion of pure Mg as a function of grain size and processing route. Adv Eng Mater 10(6):579–582

Patsalas P, Charitidis C, Logothetidis S (2000) The effect of substrate temperature and biasing on the mechanical properties and structure of sputtered titanium nitride thin films. Surf Coat Technol 125(1–3):335–340

Pawlak W, Wendler B (2009) Multilayer, hybrid PVD coatings on Ti6Al4V titanium alloy. J Achiev Mater Manuf Eng 37(2):660–667

Pohrelyuk IM, Tkachuk OV, Proskurnyak RV (2013) Corrosion behaviour of Ti–6Al–4V alloy with nitride coatings in simulated body fluids at 36 °C and 40 °C. ISRN Corros. 2013:241830

Rihawy MS, Ismail IM, Halloum D (2016) Setting up of in-vacuum PIXE system for direct elemental analysis of thick solid environmental samples. Appl Radiat Isot 110:164–173

Rizzo A, Signore MA, De Riccardis MF, Capodieci L, Dimaio D, Nocco T (2007) Influence of growth rate on the structural and morphological properties of TiN, ZrN and TiN/ZrN multilayers. Thin Solid Films 515(17):6665–6671

Roessler S, Zimmermann R, Scharnweber D, Werner C, Worch H (2002) Characterization of oxide layers on Ti6Al4V and titanium by streaming potential and streaming current measurements. Colloids Surf B 26(4):387–395

Scherrer P (1918) Determination of the size and internal structure of colloidal particles using X-rays. Nachr Ges Wiss Gottingen 26:98–100

Subramanian B, Muraleedharan CV, Ananthakumar R, Jayachandran M (2011) A comparative study of titanium nitride (TiN), titanium oxy nitride (TiON) and titanium aluminum nitride (TiAlN), as surface coatings for bio implants. Surf Coat Technol 205(21–22):5014–5020

Torres AEB, Neves SB, Abreu JCN, Cavalcante CL Jr, Ruthven DM (2001) Single- and multi-component liquid phase adsorption measurements by headspace chromatography. Braz J Chem Eng 18:121–125

Unal O, Cahit Karaoglanli A, Varol R, Kobayashi A (2014) Microstructure evolution and mechanical behavior of severe shot peened commercially pure titanium. Vacuum 110:202–206

Variola F, Yi J-H, Richert L, Wuest JD, Rosei F, Nanci A (2008) Tailoring the surface properties of Ti6Al4V by controlled chemical oxidation. Biomaterials 29(10):1285–1298

Wang T, Yu J, Dong B (2006a) Surface nanocrystallization induced by shot peening and its effect on corrosion resistance of 1Cr18Ni9Ti stainless steel. Surf Coat Technol 200(16–17):4777–4781

Wang ZB, Lu J, Lu K (2006b) Wear and corrosion properties of a low carbon steel processed by means of SMAT followed by lower temperature chromizing treatment. Surf Coat Technol 201(6):2796–2801

Wang L, Su JF, Nie X (2010) Corrosion and tribological properties and impact fatigue behaviors of TiN- and DLC-coated stainless steels in a simulated body fluid environment. Surf Coat Technol 205(5):1599–1605

Yamada M (1996) An overview on the development of titanium alloys for non-aerospace application in Japan. Mater Sci Eng, A 213(1–2):8–15

Yildiz F, Yetim AF, Alsaran A, Efeoglu I (2009) Wear and corrosion behaviour of various surface treated medical grade titanium alloy in bio-simulated environment. Wear 267(5–8):695–701

Zhang C, Song W, Li F, Zhao X, Wang Y, Xiao G (2015) Microstructure and corrosion properties of Ti–6Al–4V alloy by ultrasonic shot peening. Int J Electrochem Sci 10:9167–9178